Electronic supplementary information (ESI)

Robust and promising hydrogen and oxygen evolution reaction by nanostructured bifunctional FeCoPd alloy electrocatalyst

Ankur Kumar,[a] Siddhartha K. Purkayastha,[b] Ankur K. Guha,[c] Manash R. Das,[d] Sasanka Deka*,[a]

[a]Department of Chemistry, University of Delhi, North Campus, Delhi-110007, India

[b]Department of Chemistry, Assam Don Bosco University, Sonapur 782402, India

[c]Advanced Computational Chemistry Centre, Cotton University, Panbazar, Guwahati, Assam, India-781001

[d]Materials Sciences and Technology Division, CSIR-North East Institute of Science and Technology, Jorhat 785006, Assam, India.

Email: sdeka@chemistry.du.ac.in

Additional control syntheses

Synthesis of FeCoPd-O (FCP-O) NPs. The controlled synthesis of FeCoPd–O nanoparticles was carried out in the absence of hydrothermal treatment and without the addition of hydrazine hydrate while the rest procedure remains similar to the synthesis of FCP NPs.

Synthesis of FeCoPd-H (FCP-H) NPs. The controlled synthesis of FeCoPd-H nanoparticles was carried out in a similar manner as that of FCP nanoparticles but in the absence of hydrazine hydrate.

Synthesis of FeCoPd-1.5 (FCP-1.5) and FeCoPd-3.0 (FCP-3.0) NPs. The controlled synthesis of FeCoPd-1.5 and FeCoPd-3.0 nanoparticles were carried out in a similar manner as that of FCP nanoparticles, but with the addition of 1.5 mL and 3.0 mL of hydrazine hydrate instead of 4.5 mL as taken for FCP sample, respectively.

Synthesis of FeCoPd-N (FCP-N) NPs. The controlled synthesis of FeCoPd-N NPs (less Cl^-) was carried out in a similar manner as that of FCP nanoparticles, but $Fe(NO_3)_3.9H_2O$ and $Co(NO_3)_2.6H_2O$ salts were used in place of chloride salts.

Synthesis of FeCoPd–0.5KCl (FCP-0.5KCl) and FeCoPd–1.0KCl (FCP-1.0KCl) samples. The synthesis of FeCoPd–0.5KCl and FeCoPd–1.0KCl (more Cl^-) were carried out with the addition of 0.5 mmol and 1.0 mmol KCl solution in 7 mL of double distilled water followed by the addition of $FeCl_3.6H_2O$ (0.5 mmol), $PdCl_2$ (0.5 mmol) and $CoCl_2.6H_2O$ (0.5 mmol) before the addition of hydrazine hydrate, respectively. The remaining synthesis steps persist similar to that of FCP NPs route.

Chlorine estimation method

(Mohr's titration method)**:** https://www.canterbury.ac.nz/media/documents/science-outreach/chloride_mohr.pdf)

Preparation of 500 ppm solution of different samples containing different content of chlorine (FCP, FCP-N, FCP-0.5KCl, and FCP-1.0KCl) in a 50 mL volumetric flask. To be estimated samples first digested in an acidic medium for the complete dissolution of solid particles. Preparation of 5000 ppm solution of silver nitrate in 100 mL of volumetric flask. The indicator used in the titration was potassium chromate solution (1g of K_2CrO_4 in 20 mL of distilled water. Pipette out 10 mL of 500 ppm solution of different content of chlorine sample in 30 mL vial with the addition of 1 mL K_2CrO_4 indicator. The resultant solution was then titrated with silver nitrate solution from the burette dropwise until the color changed from cloudy faint lemon-yellow to red-brown. The estimated amount of chlorine is determined from the volume of silver nitrate used from the burette.

Instrumentation: Talos Thermo Scientific transmission electron microscope employed at accelerating voltage of 200 kV utilized for capturing transmission electron microscopy (TEM) and phase-contrast high-resolution TEM (HRTEM) images. X-ray diffraction (XRD) patterns were used to investigate the purity and crystalline phase on a Rigaku ULTIMA IV X-ray diffractometer by using Cu Kα radiation (λ = 1.54056 Å) source. Field-Emission scanning electron microscope (FESEM, JEOL JSM 6610, 20 kV) paired with Energy dispersive X-ray spectrometer has been used to examine the three-dimensional morphology and elemental

composition of the synthesized alloy samples. SEM and EDAX estimations were obtained with a JOEL JSM 6610 instrument at 20 kV, with a spot size of 35 and a width of 10 mm. X-ray Photoelectron Spectroscopy (XPS) measurements were performed on a Thermo-Scientific ESCALAB Xi+ spectrometer with a monochromatic Al Kα X-ray source (1486.6 eV) containing a spherical energy analyzer that operates in the constant analyzer energy (CAE) mode using the electromagnetic lens mode. The Nova Touch LX2 gas sorption analyzer from Quantachrome Instruments was used for analyzing BET surface area and pore size analyses. Elemental percentages were analysed in Agilent ICP-MS 7900 Inductively Coupled Plasma Mass Spectrometry (ICP-MS). Computational calculations were performed using Gaussian16 suite of program.[1]

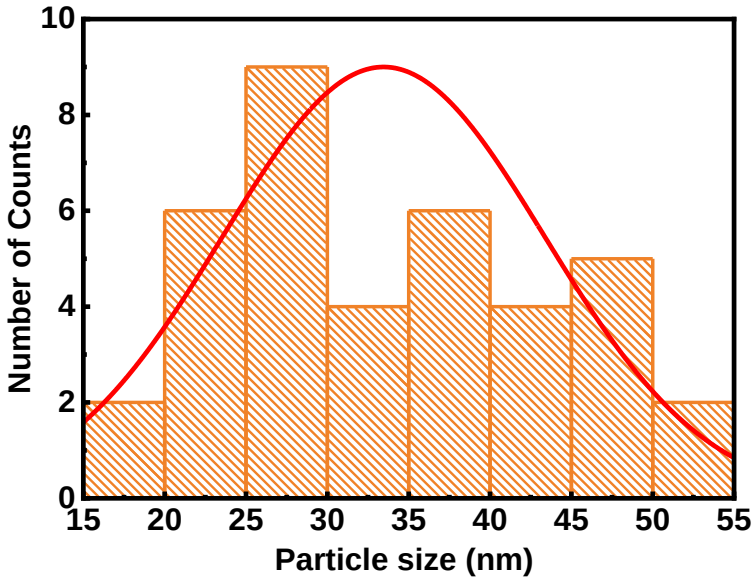

Fig. S1. Particle size distribution histograms of FCP polyhedral nanoparticles.

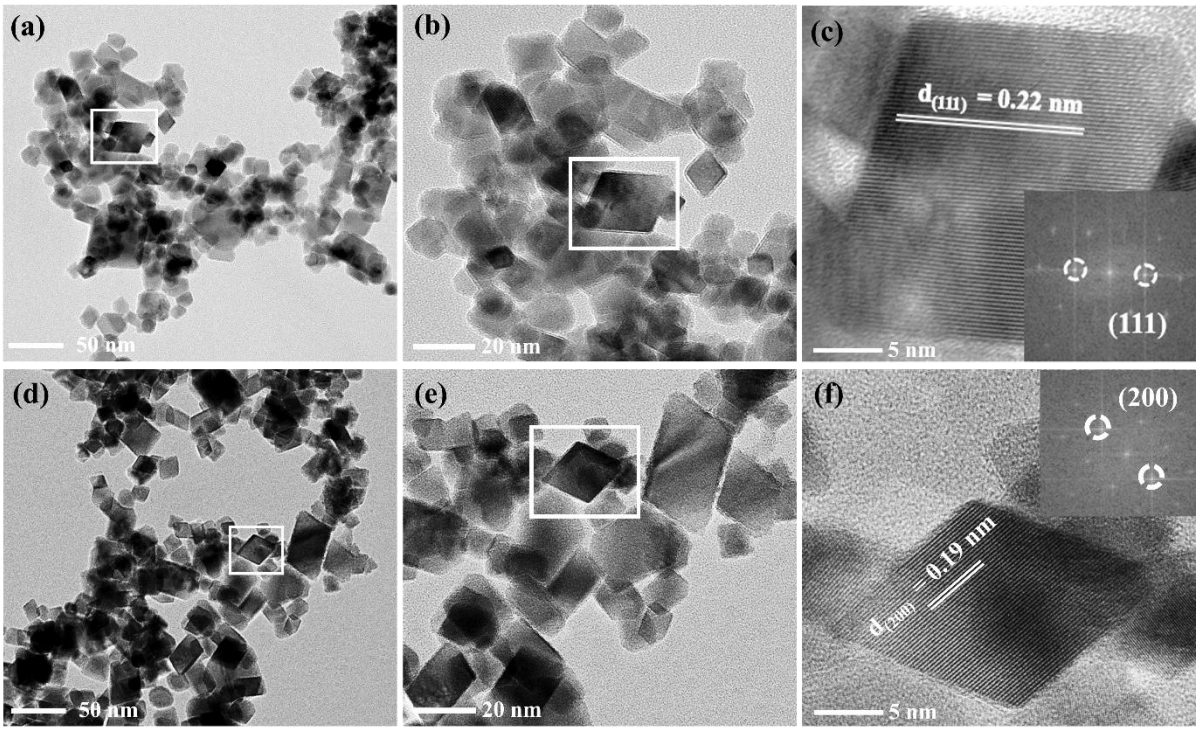

Fig. S2. (a,b and d,e) Low-and High-resolution TEM images of as-synthesized trimetallic FeCoPd nanoparticles respectively. (c and f) HRTEM image of FeCoPd polyhedral nanoparticles with (111) and (200) planes respectively. Inset: corresponding calculated 2D-FFT pattern.

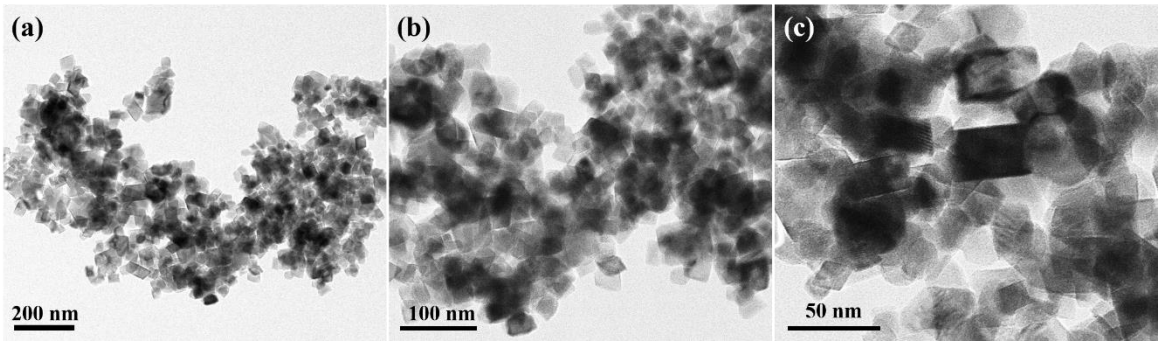

Fig. S3. (a-c) TEM images of the FCP-N sample prepared from nitrate salt of Fe and Co.

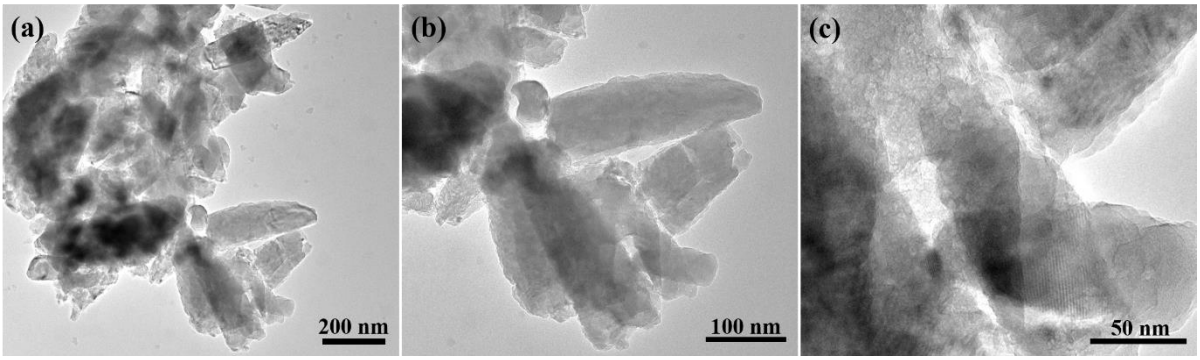

Fig. S4. (a-c) TEM images of the FCP-0.5KCl sample.

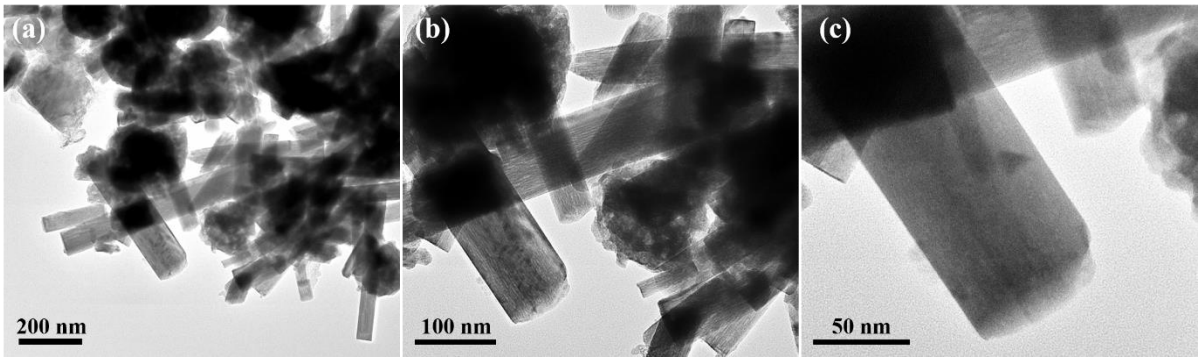

Fig. S5. (a-c) TEM images of the FCP-1.0KCl sample.

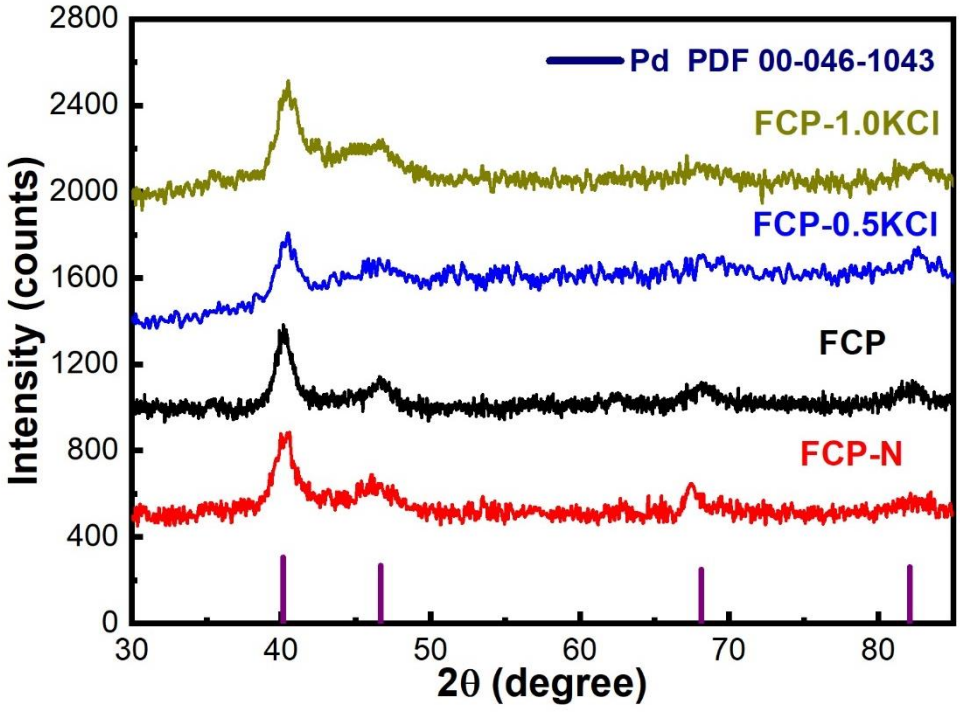

Fig. S6. X-ray diffraction patterns of the different amount of chlorine sample in FCP sample.

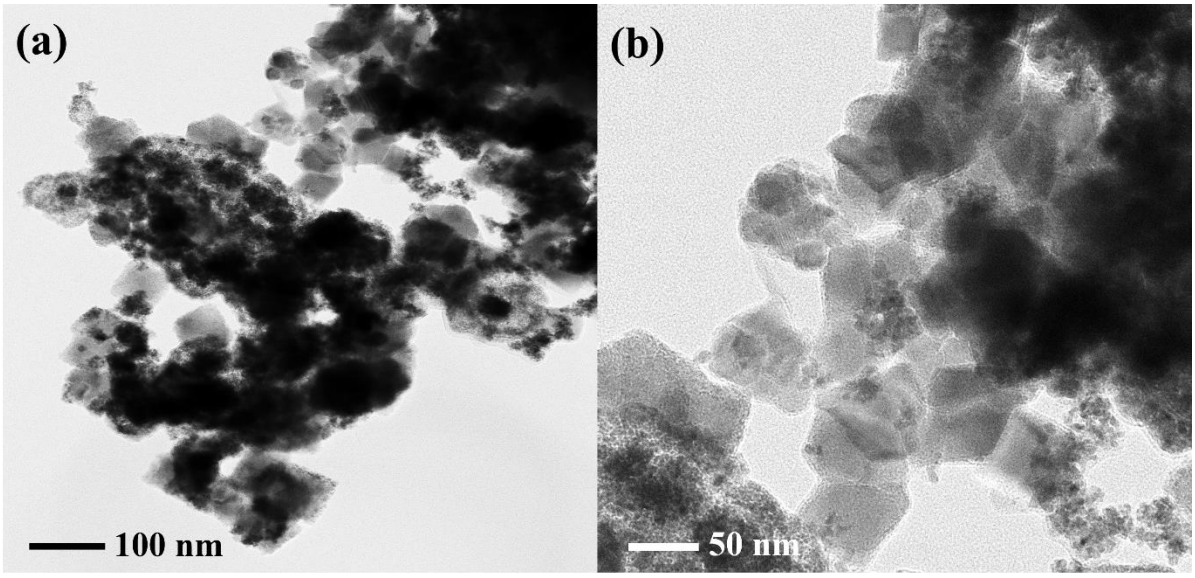

Fig. S7. (a) Low and (b) High-resolution TEM image of FeCoPd at 120˚ C.

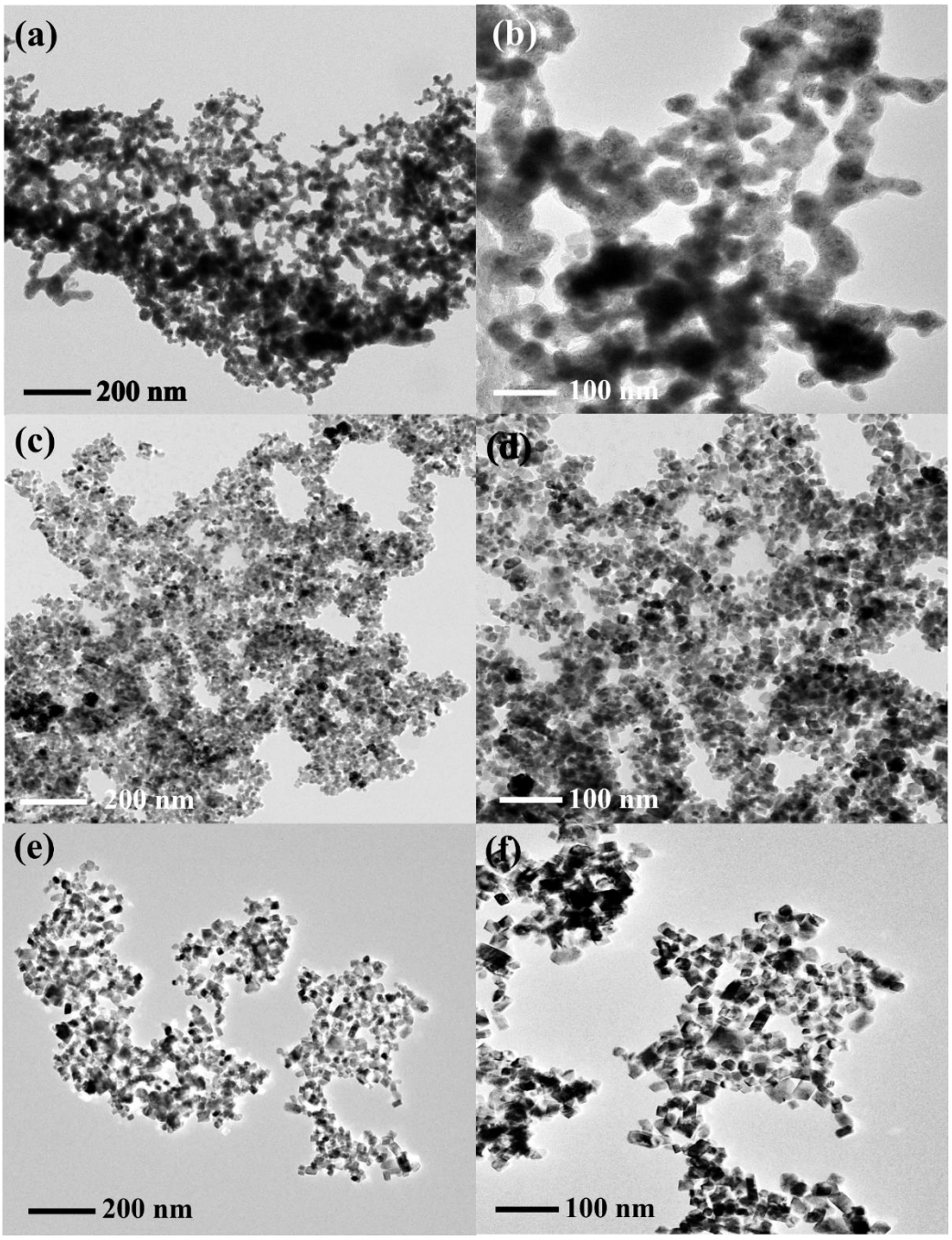

Fig. S8. Low-resolution TEM images of (a,b) CoPd, (c,d) FePd, and (e,f) FeCo NPs.

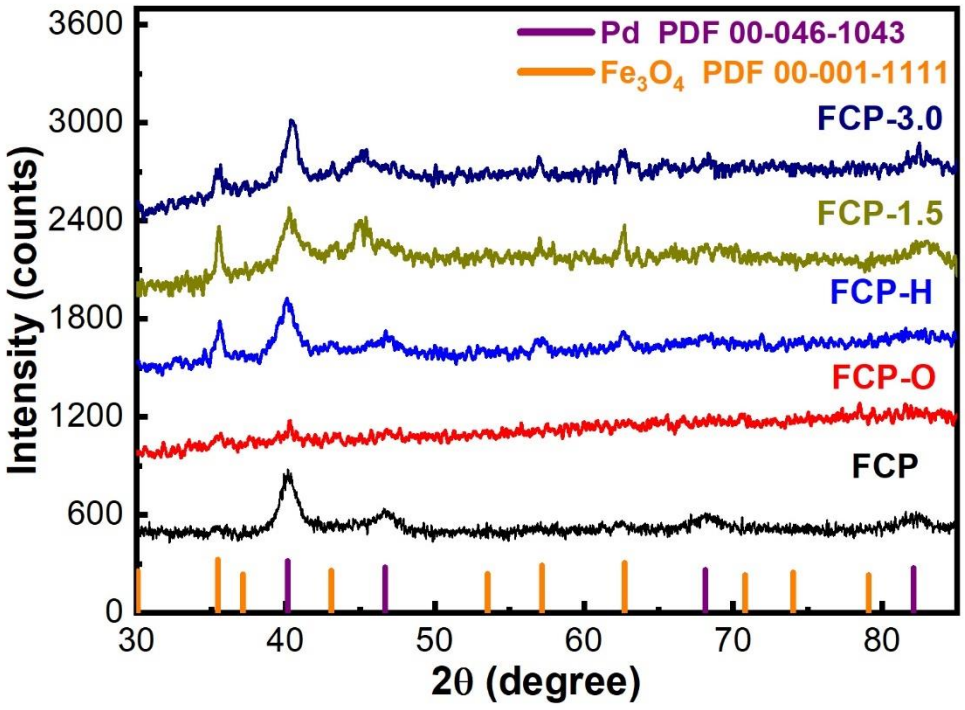

Fig. S9. Powder X-ray diffraction patterns of the controlled study of FCP sample

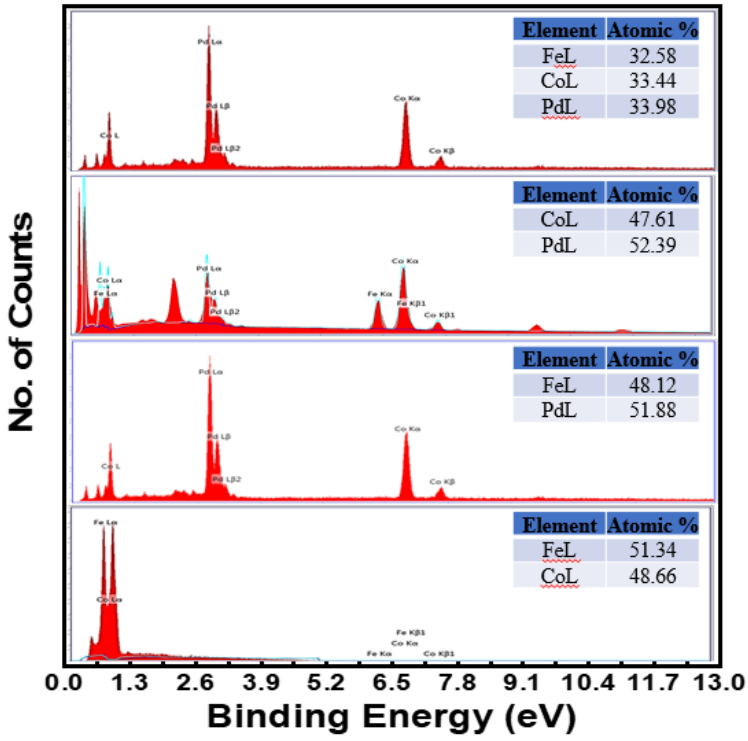

Fig. S10. SEM-EDAX survey of FCP, CP, FP, and FC samples with corresponding elemental composition.

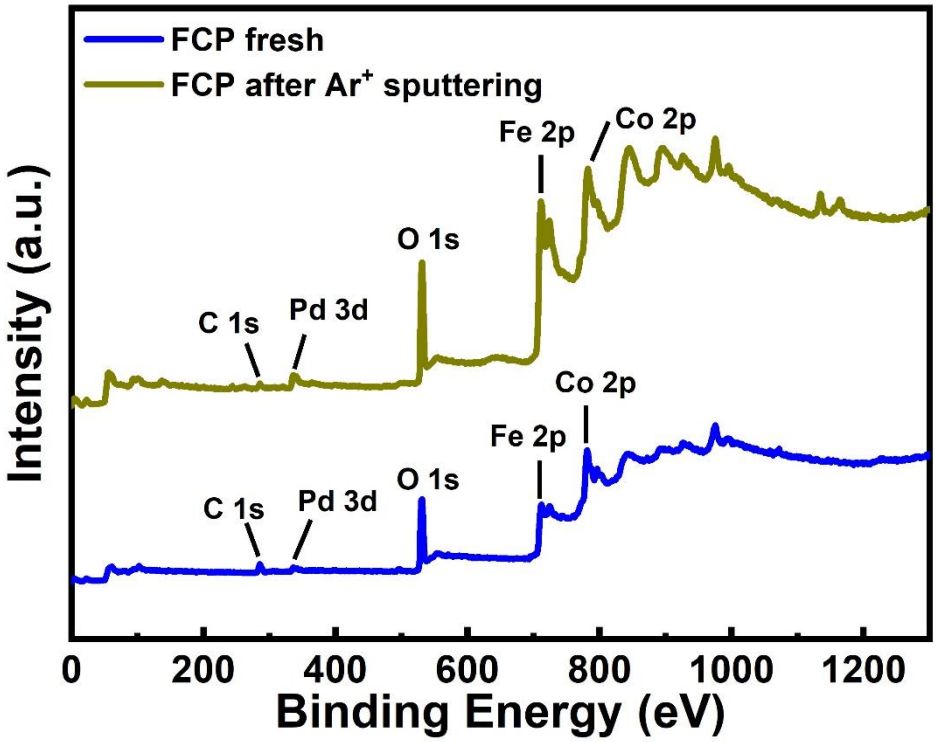

Fig. S11. Wide scan XPS spectrum of FCP fresh sample and after Ar^+ sputtering for 120s.

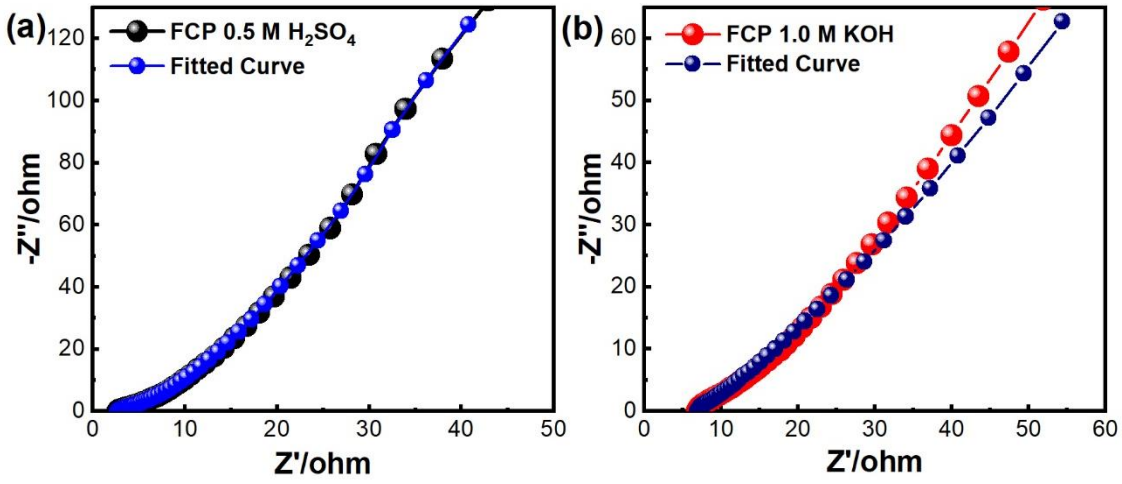

Fig. S12. Fitted curve obtained from Nyquist plot in (a) acidic and (b) alkaline electrolyte**.**

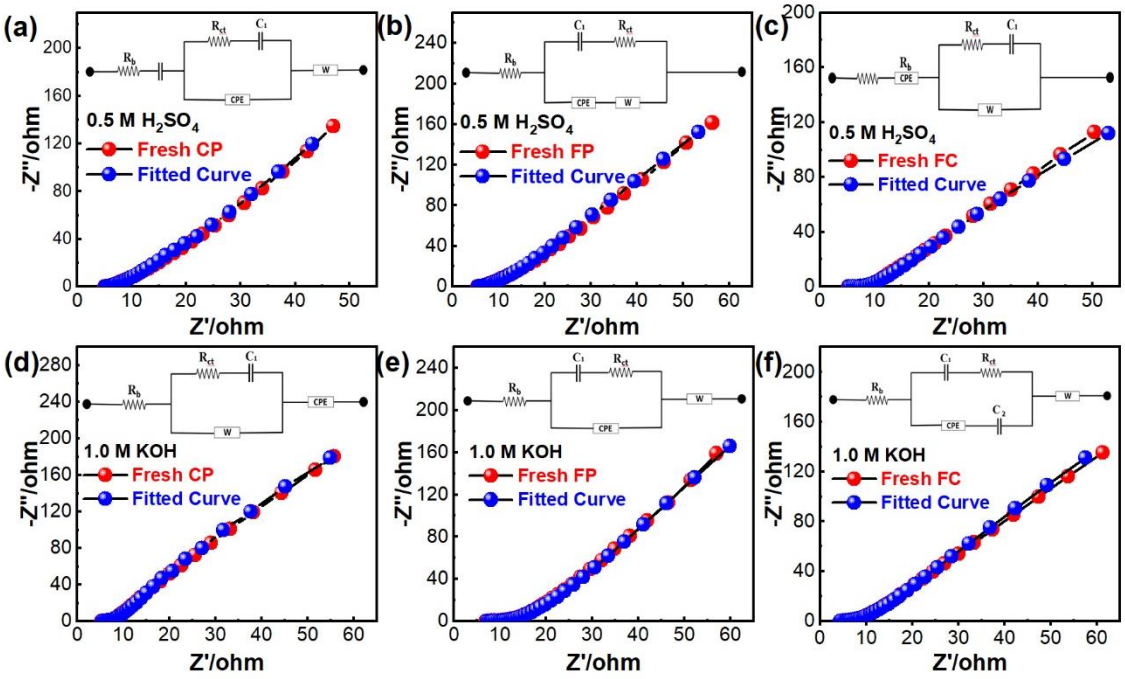

Fig. S13. Fresh and fitted curve obtained from Nyquist plot with circuit diagram corresponding to (a and d) CP, (b and e) FP, and (c and f) FP in acidic and alkaline medium respectively.

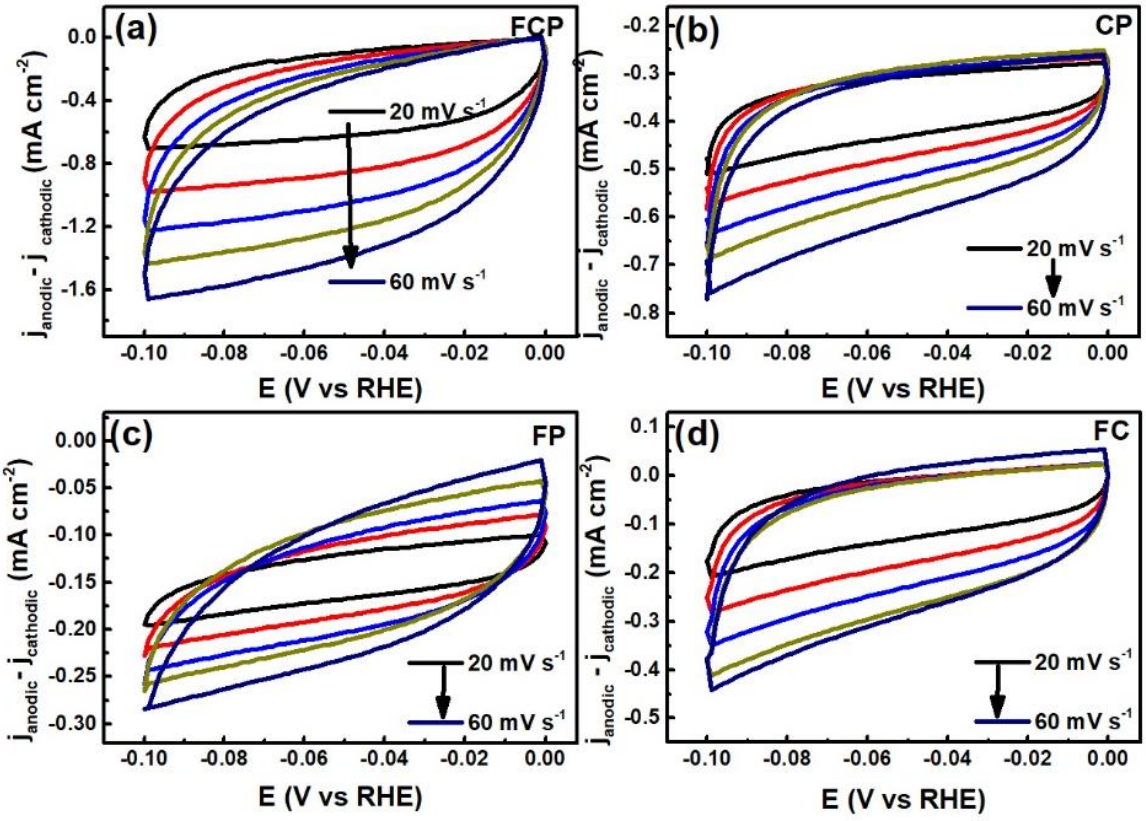

Fig. S14. CV curves at different scan rates in non-faradaic potential region in 0.5 M H_2SO_4 for (a) FCP, (b) CP, (c) FP and (d) FC samples.

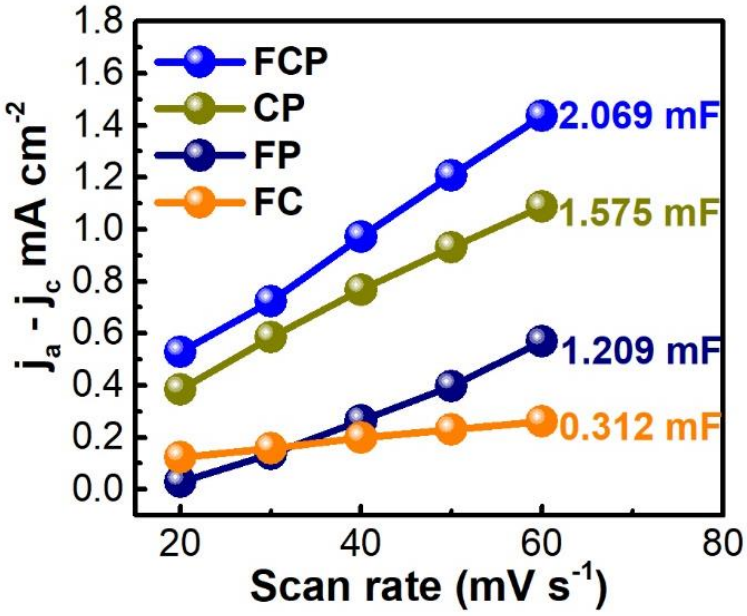

Fig. S15. Current (Δj) vs. scan rate plot in 0.5 M H_2SO_4 electrolyte.

Calculations:

1. **Exchange current density:**

Exchange current density (i_{ex}) = RT/nFΘA

Where R is the universal gas constant (8.314 J K^{-1} mol^{-1}), T is the reaction temperature (298 K), n is the number of electrons, F is the Faraday constant (96485C mol^{-1}), Θ is the charge transfer resistance calculated from EIS equivalent circuit diagram (for FCP Θ is 0.97 Ω), and A is the area of the graphite sheet electrode (0.09 cm^2).[2]

(a) In 0.5 M H_2SO_4

$$= \frac{8.314\ \text{J K}^{-1}\ \text{mol}^{-1} * 298\text{K}}{2 * 96485\ \text{C mol}^{-1} * 0.97\ \Omega * 0.09\ \text{cm}^2}$$

$$= 147.07\ \text{mA cm}^{-2}$$

(b) In 1 M KOH

$$= \frac{8.314\ \text{J K}^{-1}\ \text{mol}^{-1} * 298\text{K}}{4 * 96485\ \text{C mol}^{-1} * 1.55\ \Omega * 0.09\ \text{cm}^2}$$

$$= 46.02\ \text{mA cm}^{-2}$$

2. Mass activity:[3]

Mass activity (A/g) = j/m

Where j is the current density (mA cm^{-2}) and m is mass loading onto graphite sheet working electrode (mg cm^{-2})

$$= \frac{10 \text{ mA cm}^2}{2.14 \text{ mg cm}^{-2}}$$

$$= 4.67 \text{ A g}^{-1}$$

3. Turn over frequency (TOF) calculation:[4,5]

$$\text{Turn over frequency (TOF)} = \frac{\text{j X A}}{\text{n X F X N}_s}$$

Where j is the current density (mA cm^{-2}), *A* is the area of the electrode (cm^{-2}), *F* is the Faraday constant (96,485 C mol^{-1}) and N_s is the concentration of active sites in the catalysts (mol cm^{-2}). To calculate N_s, cyclic voltammetry (CV) was performed for in non-Faradaic region at different scan rates in 0.5 M H_2SO_4 and 1.0 M KOH electrolytes. The peak currents were plotted versus scan rates where the slope is equal to

$$\text{Slope} = \frac{F^2AN_s}{nRT}$$

$N_s = 1.101 \times 10^{-9}$ mol (0.5 M H_2SO_4)

$N_s = 4.160 \times 10^{-9}$ mol (1.0 M KOH)

where n is the number of electrons transferred, F presents the Faradic constant, A is the surface area of the electrode, *Ns* is the surface concentration of active sites (mol), R and T is the ideal gas constant and the absolute temperature, respectively.

$$\text{TOF (0.5 M } H_2SO_4) = \frac{10 \text{ mA cm}^{-2} \times 0.09 \text{ cm}^2}{2 \times 96{,}485 \text{ C mol}^{-1} \times 1.101 \times 10^{-9} \text{ mol}}$$

$$= 4.23 \text{ s}^{-1}$$

$$\text{TOF (1.0 M KOH)} = \frac{10 \text{ mA cm}^{-2} \times 0.09 \text{ cm}^2}{4 \times 96{,}485 \text{ C mol}^{-1} \times 4.160 \times 10^{-9} \text{ mol}}$$

$$= 0.56 \text{ s}^{-1}$$

4. Electrochemical active surface area (ECSA):

The Electrochemical active surface area was calculated from double-layer capacitance of modified catalyst electrode in 1.0 M KOH.[6] The slope of curve ΔJ ($J_{anodic} - J_{cathodic}$/ $mAcm^{-2}$) versus Scan rate (mV s^{-1}) give the value of $2C_{dl}$.[4]

$$ECSA = C_{dl}/C_s$$

Where C_{dl} is the measured double layer capacitance and C_s is the specific capacitance of the catalyst (0.04 mF cm^{-2} in 1.0 M KOH)

$$= \frac{1.954\ \text{mF}}{0.04\ \text{mF cm}^{-2}}\ \ (1.0\ \text{M KOH})$$

$$= 48.85\ \text{cm}^2$$

5. Theoretically calculated amount of oxygen

The theoretical amount of expected total gas volume was evaluated using Faraday's law of electrolysis with the ideal gas law:[7]

$$V_{theo} = \frac{RT}{F\ p\ z}Q$$

Here, *R* is the ideal gas constant, *T* is the absolute temperature, *Q* is the charge (at an applied current density of 50 mA cm^{-2} for 60 minutes), *F* is Faraday's constant, *p* is the pressure and *z* = 4 is the number of electrons involved.

Table S1. Summary of overpotential (mV) and Tafel slope (mV dec^{-1}) of the studied catalysts.

Sr. No.	Catalysts (code)	Overpotential (mV)		Tafel slope (mV dec^{-1})	
		HER (0.5 M H_2SO_4)	OER (1 M KOH)	HER (0.5 M H_2SO_4)	OER (1 M KOH)
1.	IrO_2	-	295	-	92
2.	Pt/C	36	-	35	-
3.	FCP/GS	52	197	38	47
4.	CP/GS	79	290	55	88
5.	FP/GS	85	328	71	130
6.	FC/GS	213	270	125	84

Table S2. Comparison of the electrocatalytic HER activity of the present FeCoPd with other reported electrocatalysts in acidic electrolyte.

Sr. No.	**Catalysts**	**Substrate**	**Over potential (mV) at 10 mA cm^{-2}**	**Tafel Slope (mV dec^{-1})**	**Durability (h)**	**Reference**
1	FCP (FeCoPd)	GS	52	38	66	This Work
2	$Ir_{25}Ni_{33}Ta$	Si	99	35	10	Adv. Mater.2019, 1906384
3	$Pd_{50}Ag_{50}$	NF	97	75.5	20000 seconds	Int. J. Electrochem. Sci., 2019, 14, 8781-8792
4	PdCu@Pd NCs	GC	65	35	-	ACS Appl. Mater. Interfaces, 2017, 9, 8151-8160
5	Ni/WC@NC	GC	53	43.5	24	Energy Environ. Sci., 2018, 11, 2114-2123
6	RuNi/CQDs-600	GC	58	55	100	Angew. Chem. Int. Ed., 2019, 59, 1718-1726
7	$Ni_{0.8}Fe_{0.2}Se_2$	GC	64	43	4500 sec	Nano Res., 2018, 11, 6051-6061

8	Pd-CN_X	GC	55	35	100	ACS Catal., 2016, 6, 1929-1941
9	Ni_3Cu_1NG -NC	GC	95	77.1	-	Small, 2019, 15, 1901545
10	Co_9S_8	GC	71	42.4	10	J. Colloid Interface sci., 558(2020) 155-162
11	VGN@$Pd_{0.2}$-MoS_2	CFP	106	60	1100	J. Power Sources 456 (2020) 227998
12	CoP/NiCoP	GC	60	64	80	Adv. Func. Mater., 2018, 29, 1807976
13	MoP/MoS_2	CC	69	61	24	ACS Appl. Mater. Interfaces, 2019, 11, 25986-25995
14	CuPdPt/C	GC	55	25	8000 seconds	J. Mater. Chem. A, 2016, 4, 15309-15315
15	PtCu/CNFs	CNF	71	68	10	Adv. Mater. Interfaces 2017 1700005

16	PdCo@CN	GC	80	31	40000 seconds	ACS Appl. Mater. Interfaces 2016, 8, 13378

Table S3. Summary of Charge transfer resistance and Exchange current density of the studied catalysts.

Sr. No.	**Catalysts (code)**	**Charge transfer resistance (R_{ct}, ohm)**		**Exchange current density (i_{ex}/mA cm^{-2})**	
		0.5 M H_2SO_4	**1 M KOH**	**0.5 M H_2SO_4**	**1 M KOH**
1.	FCP/GS	0.97	1.55	147.07	46.02
2.	CP/GS	1.69	3.37	84.41	21.16
3.	FP/GS	1.99	6.53	71.69	10.92
4.	FC/GS	3.67	2.69	38.87	26.52

Table S4. Summary of TOF (s^{-1}) and ECSA (cm^2) of the studied catalysts.

Sr. No.	**Catalysts (code)**	**TOF (s^{-1})**		**ECSA (cm^2)**
		0.5 M H_2SO_4	**1 M KOH**	**1 M KOH**
1.	FCP/GS	4.23	0.56	48.85
2.	CP/GS	2.7	0.51	16.15
3.	FP/GS	2.51	0.44	6.65
4.	FC/GS	1.57	0.52	43.62

Table S5. Comparison of the electrocatalytic OER activity of the present FeCoPd with other reported electrocatalysts in alkaline electrolyte.

Sr. No.	**Catalysts**	**Substrate**	**Over potential (mV) at 10 mA cm^{-2}**	**Tafel Slope (mV dec^{-1})**	**Durability (h)**	**Reference**
1	FCP (FeCoPd)	GS	197	47	100	This Work
2	$Ni_{2.5}Co_{0.5}Fe$	NF	275	105	-	J. Mater. Chem. A, 2016, 4, 7245-7250
3	NiFeMo	NF	238	60	50	ACS Energy lett. 2018,3,546-554
4	FeCoNi	GC	288	-	10	ACS Catal. 2017, 7, 469-479
5	$Ir_{44}Pd_{10}$	GC	226	53.9	15	Angew. Chem. Int. Ed., 2019, 58, 7244-7248
6	Y-S Ni-Co-Se	CFP	300	72	18	ACS Sustain. Chem. Eng. 2018, 6, 10952-10959
7	Ru_1Co_2	CC	240	54.4	10	ACS Appl. Energy Mater. 2020 , 3, 2, 1869–1874

8	Fe_2Co-MOF	GC	339	36.2	-	Inorg. Chem. 2020, 59, 9, 6078–6086
9	$NiRuO_X$@C	RDE	252	62	12	Chem. Eng. J., 2021, 426, 130762.
10	RuCo@CDs	GC	257	96.1	20	J. Mater. Chem. A, 2020,8, 9638-9645
11	$Ir_{0.5}W_{0.5}$	GC	281 (0.1 M KOH)	52	30000 sec	Nanoscale, 2019,11, 8898-8905
12	RuNi NAs	GC	304	73.4	10	iScience, 2019, 11, 492-504
13	$RuTe_2$ PNRs	GC	285	62	-	Nat. Commun., 2019, 10
14	NiCo-UMOFNs	GC	250	42	-	J. Mater. Chem. A, 2018, 6, 22070-22076
15	Li-$IrSe_2$	GC	270	-	10	Angew. Chem. Int. Ed. Engl. 2019 14764-14769.
16	$RuIrO_x$	CFP	250	50	-	Nature Communications 2019, 10, 4875

17	$Ni_{0.93}Ir_{0.07}$/ rGO	CFP	271.8	55.9	13	J. Energy Chem. 2020, 49, 166-173

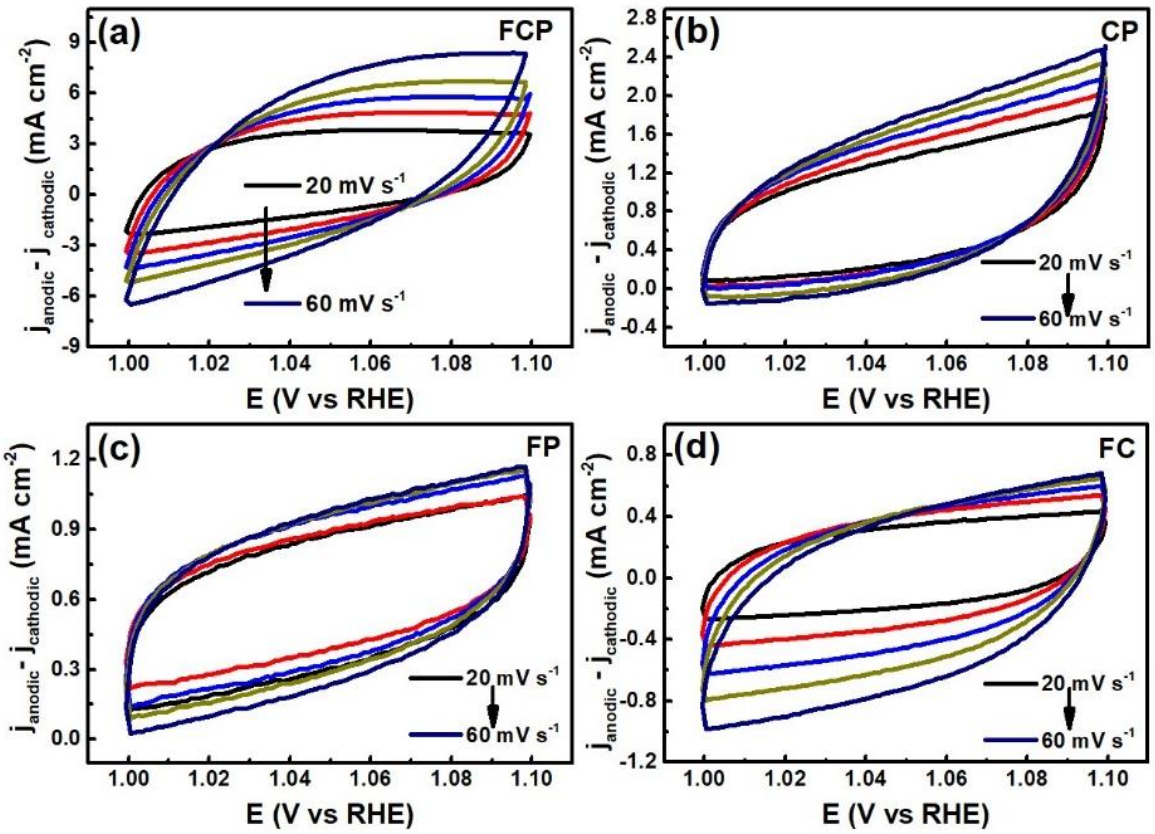

Fig. S16. CV curves at different scan rates in non-faradaic potential region in 1.0 M KOH for (a) FCP, (b) CP, (c) FP and (d) FC samples.

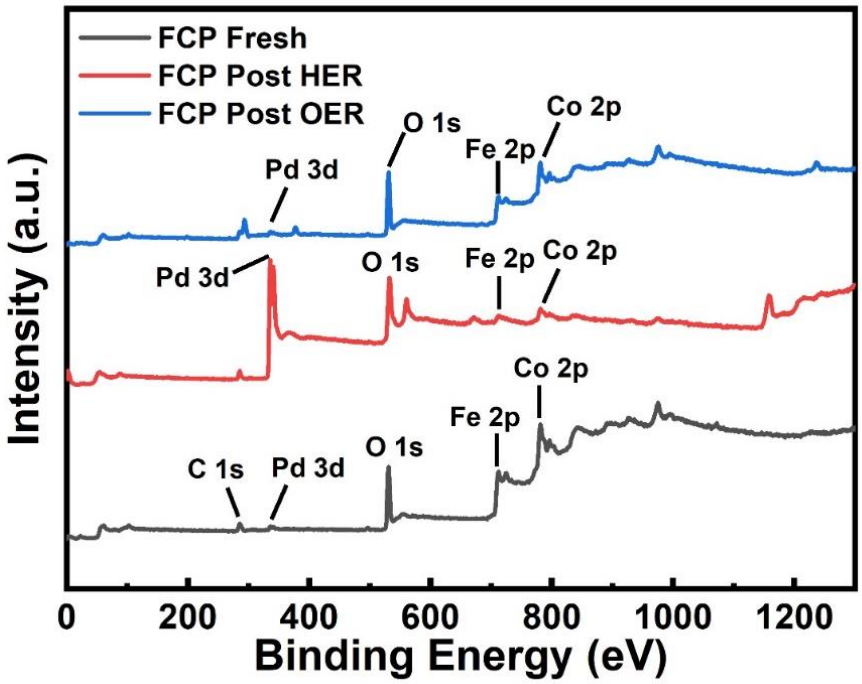

Fig. S17. Wide scan XPS spectrum of Fresh FCP, FCP Post HER and FCP Post OER samples.

Table S6. Elemental concentration (%) analysed by ICP-MS before and after the stability tests.

Sample Name	**Sample wt. (g)**	**Volume makeup (mL)**	**Conc. (g/L)**	**Fe Conc. (µg/g)**	**Co Conc. (µg/g)**	**Pd Conc. (µg/g)**
FCP	0.0974	40	2.435	150826.28	169220.12	166128.13
FCP Post HER	0.0971	40	2.4275	157312.04	172381.05	167335.94
FCP Post OER	0.0974	40	2.435	145282.54	170673.10	170030.80

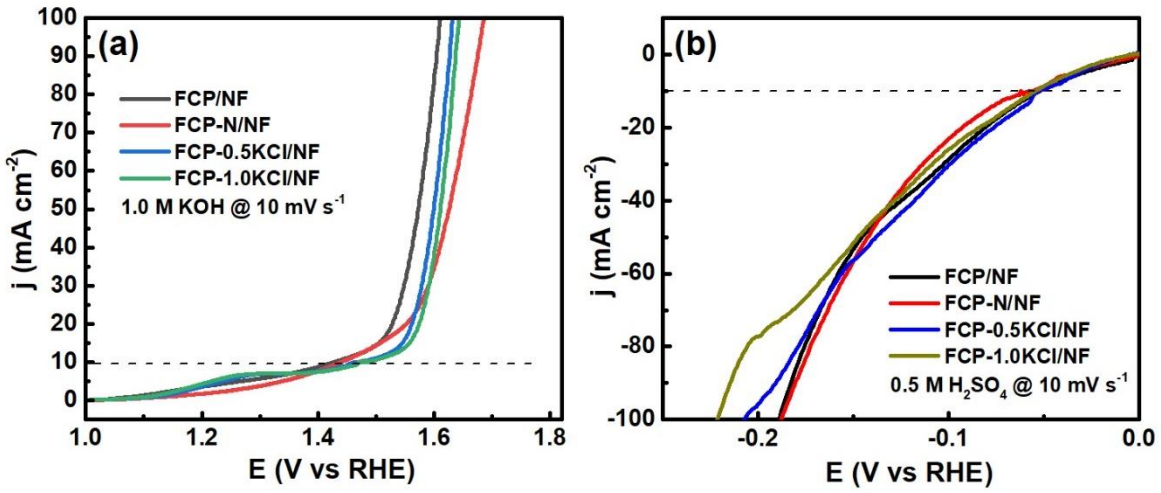

Fig. S18. (a) OER and (b) HER LSV polarisation curves of different contents of the chlorine in FCP sample.

Table S7 Adsorption free energy $H(\Delta G(H^*))$ of (in eV) for bimetallic and trimetallic alloys.

Structure	**$\Delta G(H^*)$**
FP	0.38
FC	1.21
CP	0.29
FCP	-0.08

References.

1. Gaussian 16, Revision B.01, M. J. Frisch, G. W. Trucks, H. B. Schlegel, G. E. Scuseria, M. A. Robb, J. R. Cheeseman, G. Scalmani, V. Barone, G. A. Petersson, H. Nakatsuji, X. Li, M. Caricato, A. V. Marenich, J. Bloino, B. G. Janesko, R. Gomperts, B. Mennucci, H. P. Hratchian, J. V. Ortiz, A. F. Izmaylov, J. L. Sonnenberg, D. Williams-Young, F. Ding, F. Lipparini, F. Egidi, J. Goings, B. Peng, A. Petrone, T. Henderson, D. Ranasinghe, V. G. Zakrzewski, J. Gao, N. Rega, G. Zheng, W. Liang, M. Hada, M. Ehara, K. Toyota, R. Fukuda, J. Hasegawa, M. Ishida, T. Nakajima, Y. Honda, O. Kitao,

H. Nakai, T. Vreven, K. Throssell, J. A. Montgomery, Jr., J. E. Peralta, F. Ogliaro, M. J. Bearpark, J. J. Heyd, E. N. Brothers, K. N. Kudin, V. N. Staroverov, T. A. Keith, R. Kobayashi, J. Normand, K. Raghavachari, A. P. Rendell, J. C. Burant, S. S. Iyengar, J. Tomasi, M. Cossi, J. M. Millam, M. Klene, C. Adamo, R. Cammi, J. W. Ochterski, R. L. Martin, K. Morokuma, O. Farkas, J. B. Foresman, and D. J. Fox, Gaussian, Inc., Wallingford CT, 2016.

2. P. Kush, K. Deori, A. Kumar and S. Deka, *J. Mater. Chem. A*, 2015, **3**, 8098-8106.
3. M. Chauhan, K. P. Reddy, C. Gopinath and S. Deka, *ACS Catal.*, 2017, **7**, 5871-5879.
4. H. Han, Y. R. Hong, J. Woo, S. Mhin, K. M. Kim, J. Kwon, H. Choi, Y. C. Chung and T. Song, *Adv. Energy Mater.*, 2019, **9**, 1803799.
5. X. Li, X. Lv, X. Sun, C. Yang, Y. Z. Zheng, L. Yang, S. Li and X. Tao, *Appl. Catal. B*, 2021, **284**, 119708.
6. X. Shang, K. L. Yan, Y. Rao, B. Dong, J. Q. Chi, Y. R. Liu, X. Li, Y. M. Chai and C. G. Liu, *Nanoscale*, 2017, **9**, 12353-12363.
7. F. Urbain, V. Smirnov, J. P. Becker, A. Lambertz, F. Yang, J. Ziegler, B. Kaiser, W. Jaegermann, U. Rau and F. Finger, *Energy Environ. Sci.*, 2016, **9**, 145-154.

******